Emission of Liquid Metal in Vacuum

G. Néron de Surgy and J.-P. Chabrerie

Laboratoire de Génie Electrique de Paris,
École Supérieure d'Électricité, Gif-sur-Yvette, France

J. E. Wesfreid

Laboratoire d'Hydrodynamique et Mécanique Physique,
Paris, France

ABSTRACT

The destabilization of an infinite plane surface of liquid metal by a normal electric field in vacuum has been the subject of different theoretical articles: above a critical field peaks grow on the liquid surface. A wavelength can be attributed to the resulting pattern. The electric field at onset and the corresponding wavelength only depend on the density and the surface tension of the liquid. Above this critical field a whole range of wavelengths are excited, each growing with a different growth time: the fastest is the dominant wavelength. We shall present the dynamics of the liquid viscosity and of the liquid bath depth: it can be shown that the dominant wavelength is smaller with higher fields but differs if the liquid film is thick or thin, inviscid or viscous. The development of the pattern involves nonlinear interactions. While a stable deformed interface has been observed on the analogous case of a magnetic fluid under magnetic field, experimentally we only found stable non-plane interface for a confined geometry where the volume conservation makes forming the destabilization more difficult: indeed the critical field for the obtainment of peaks is then greater than the value of the horizontally infinite surface. Otherwise, some peaks emit at their apex, killing the field: thus the peaks fall, do not emit any more and the electric field is installed again; this gives an oscillatory phenomenon. For a sufficiently large liquid bath different wavelengths can be seen, depending on the electric field and the way this field was reached. For confined geometries one or two peaks grow on the surface and the critical field can be significantly higher.

1. INTRODUCTION

We shall consider (Figure 1) a conducting and incompressible layer of liquid metal laying on a metallic electrode. The undisturbed free surface of the liquid is at $z = 0$ and the electrode at $z = -a$. Another electrode is placed at $z = b$, with vacuum for $0 < z < b$ and a potential V is applied between the electrodes. The geometry will first be supposed to be unbounded for both x and y.

In the following we shall denote by ρ the density of the liquid, S its surface tension, η its dynamic viscosity, $\nu = \eta/\rho$ its kinematic viscosity, by ϵ_0 the permittivity of vacuum, g the gravitational field, by $\zeta(x, y)$ the vertical displacement of the interface, $\vec{v}(x, y, z)$ the velocity of the fluid, $\vec{e}(x, y, z)$ the electric field in vacuum and by $\vec{n}(x, y)$

1070–9878/95/ $3.00

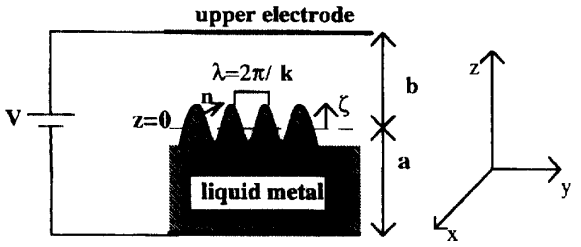

Figure 1. Principle of the experiment.

the unit vector normal to the interface.

The stability of such a film under a normal electric field $E_0 = V/b$ has already been studied in linear theory [1–8]. Nonlinear work has also been done in [9–11].

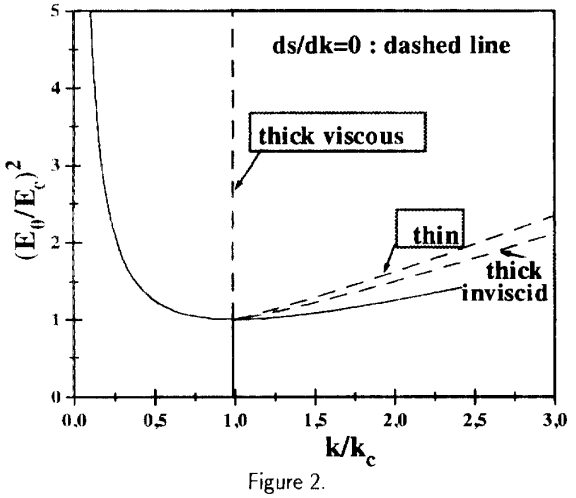

Figure 2.

Curve of marginal stability and dominant modes (for $b \gg l_c = 1/k_c$, so that $\coth(kb) = 1$).

It is known that destabilization of an unbounded liquid surface occurs only above a critical field

$$E_c = \sqrt{\frac{2}{\epsilon_0}\sqrt{\rho g S}} \tag{1}$$

for which a pattern appears, associated with a critical wavelength

$$\lambda_c = 2\pi/k_c = 2\pi l_c = 2\pi\sqrt{\frac{S}{\rho g}} \tag{2}$$

where k_c (respectively l_c) is the capillary wavenumber (respectively length). Above this field a whole range of wavelengths are excited, this range being limited by the curve of marginal stability. A linear analysis leads to a linear curve of marginal stability (Figure 2 for $b \gg l_c$), which is independent of viscosity η and fluid depth a.

We shall present the dynamics of the problem and an experimental study of the pattern where the restriction of a bounded geometry can affect the critical field value.

2. GENERAL CASE

2.1. THE EQUATIONS

The system is submitted to the following equations (for an incompressible fluid, and if η and S are constant) for $z < \zeta(x, y)$ in the liquid metal

$$\begin{aligned} \nabla \cdot \vec{v} &= 0 \\ \rho[\partial_t \vec{v} + (\vec{v} \cdot \nabla)\vec{v}] &= -\nabla p + \eta \Delta \vec{v} + \rho g \end{aligned} \tag{3}$$

and for $z > \zeta(x, y)$ in vacuum

$$\begin{aligned} \nabla \times \vec{e} &= 0 \\ \nabla \cdot \vec{e} &= 0 \end{aligned} \tag{4}$$

with the following boundary conditions where $||X|| = X_2 - X_1$ = value above the interface - value under the interface, and $1/R$ is the mean curvature of the interface (positive if towards the fluid)).

$$\begin{aligned} T_{ik} &= \epsilon_0 e_i e_k - \frac{\epsilon_0}{2} e^2 \delta_{ik} \\ \sigma'_{ik} &= \eta\,(\partial_{x_k} v_i + \partial_{x_i} v_k) \end{aligned} \tag{5}$$

For free surface condition at $z = \zeta$

$$\partial_t \zeta = v_z - v_x \partial_x \zeta - v_y \partial_y \zeta \tag{6}$$

For stress balance at the interface at $z = \zeta$

$$-||p||n_i + ||T_{ik} + \sigma'_{ik}||n_k - (S/R)n_i \tag{7}$$

For liquid metal at $z = \zeta$

$$\vec{n} \times \vec{e} = 0 \tag{8}$$

For velocity equal to zero at the electrode at $z = -a$

$$\vec{v} = \vec{0} \tag{9}$$

For electric field normal to the electrode at $z = b$

$$e_x = e_y = 0 \tag{10}$$

We limit ourselves to a linear analysis; using a Fourier expansion enables us to study the different modes separately. We therefore look at solutions with the following form

$$A(r, z, t) = A(x, y, z, t) = a(z)\exp(st - i\vec{k} \cdot \vec{r}) \tag{11}$$

It gives after some algebra the dispersion relation between the perturbation growth rate s and the wavenumber k (the modulus of the wave vector $\boldsymbol{k}$) for a field E_0

$$\begin{aligned} &4qk^3\left[q - k\coth(ka)\coth(qa)\right] - \\ &\left(q^2+k^2\right)^2\left[q\coth(ka)\coth(qa) - k\right] + \\ &\frac{4qk^2\left(q^2+k^2\right)}{\sinh(ka)\sinh(qa)} = \\ &\frac{\rho}{\eta^2}\left[Sk^3 - \epsilon_0 E_0^2\coth(kb) + \rho g k\right]\times \\ &\left[q\coth(qa) - k\coth(ka)\right] \end{aligned} \tag{12}$$

with $q^2 = k^2 + s/v$. In the case of a vanishing viscosity, Equation (3) can be simplified; we retrieve the classical result of an inviscid layer

$$\rho s_i^2 = \left[-Sk^3 + \epsilon_0 E_0^2\coth(kb)k^2 - \rho g k\right]\tanh(ka) \tag{13}$$

2.2. THE DISPERSION EQUATIONS FOR THE DIFFERENT BEHAVIORS

The hypothesis used to derive the different equations should be verified around the dominant mode $s = s_{max}$, obtained for $ds/dk = 0$, provided the potential has been applied sufficiently quickly. If the field is applied too slowly the transition will occur before the maximal potential will be reached. For a very slowly applied field the transition occurs near the critical field and once the instabilities have begun to grow, an increase of the potential will not change the wavelength of the initial stage.

The time needed to apply the potential should be smaller than the growth time $(1/s)$ if we want that $ds/dk = 0$ corresponds to the most important (dominant) mode.

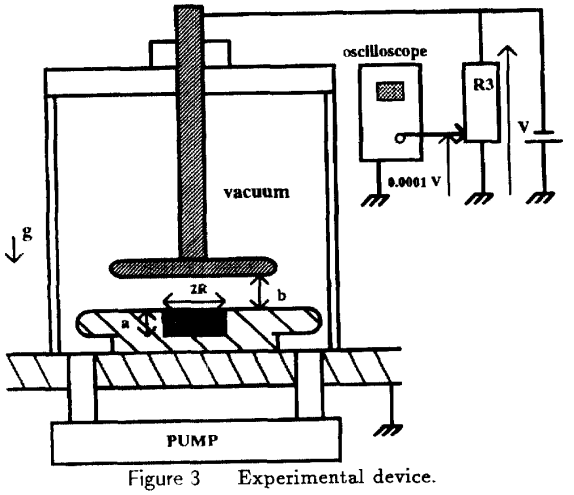

Figure 3 Experimental device.

The film is called thick if $a \gg 2\pi/\lambda$, thin if $a \ll 2\pi/\lambda$, inviscid if $s/\nu \gg \max\left(k^2, 1/a^2\right)$, and viscous if $s/\nu \ll \max\left(k^2, 1/a^2\right)$. We therefore encounter the asymptotic behavior shown in Equations (14) to (17).

Thick and inviscid

$$\rho s_{tk.i}^2 = -Sk^3 + \epsilon_0 E_0^2\coth(kb)k^2 - \rho g k \tag{14}$$

Thin and inviscid

$$\rho s_{tn.i}^2 = \left[-Sk^3 + \epsilon_0 E_0^2\coth(kb)k^2 - \rho g k\right]ka \tag{15}$$

Thick and viscous

$$s_{tk.v} = \frac{1}{2\eta}\left[-Sk + \epsilon_0 E_0^2\coth(kb) - \frac{\rho g}{k}\right] \tag{16}$$

Thin and viscous

$$s_{tn.v} = \frac{(ka)^3}{3\eta}\left[-Sk + \epsilon_0 E_0^2\coth(kb) - \frac{\rho g}{k}\right] \tag{17}$$

The curve of marginal stability is defined by $s(k) = 0$, which gives $\rho g - \epsilon_0 E_0^2 k\coth(kb) + Sk^2 = 0$, and plotted in Figure 2 with the dominant mode for each case.

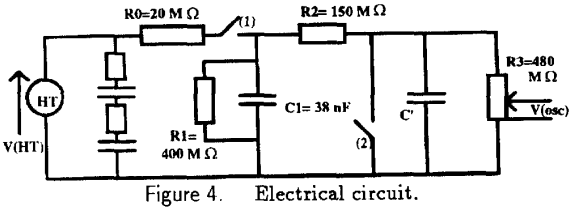

Figure 4. Electrical circuit.

3. EXPERIMENTAL STUDY OF THE PATTERN

The liquid used is mercury. As usual for liquid metals, the viscosity can be neglected, and we shall work with sufficiently thick layers, unless otherwise stated.

The experimental device is shown in Figure 3 and the electrical circuit in Figure 4. The electric field is obtained thanks to two electrodes. The value of this field is 70 kV/cm. Is well above the disruptive field of air (30 kV/cm) so that vacuum has to be used. The dc supply (Spellman dc supply) allows voltages to 110 kV. We therefore took a value of b from 0.5 to 1 cm.

The geometry of the bath is axisymmetric: the initial surface is a disk of radius R. An electrochemical treatment of the lateral boundaries has been performed, leading to an anchorage of the liquid at $r = R$. The bath is filled so that the initial surface is flat (a consequence of the electrochemical treatment is that there is no fixed contact angle), see Figure 5(a), and remains flat until the critical field (no deflection of zeroth order).

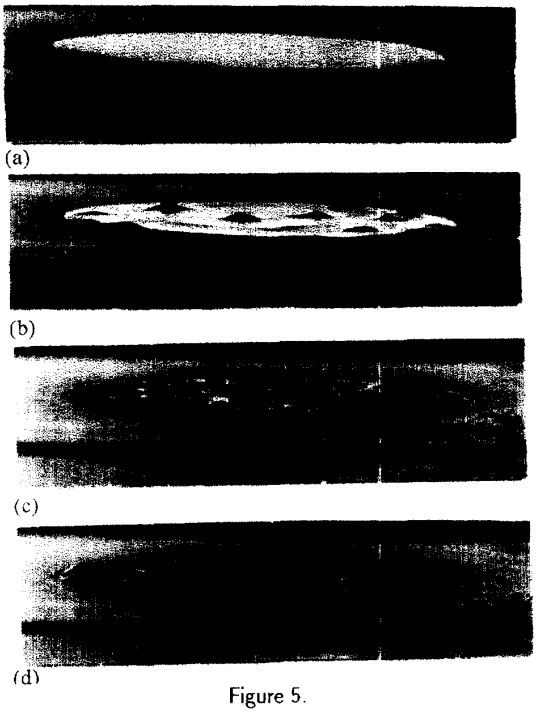

Figure 5.

Patterns in large geometry (R = 2 cm) (a) No electric field, (b) at onset, (c) above onset, (d) under the critical field after transition (hysteresis).

3.1. LATERALLY UNBOUNDED GEOMETRY

We shall first study the case of a large bath: it means that the pattern in the central part of the bath has enough place to forget the lateral boundary conditions, so the dimensions of the bath are large compared to the wavelength. The system can be considered as unbounded in the horizontal directions.

Experimentally it is difficult to observe the initial linear stage of the phenomenon. As the peaks grow further, nonlinear interactions become important and the selection of the resulting pattern, such as squares and hexagons [10, 11] is made by these interactions.

Once the peaks grow they emit at their apex when the radius of the tip is sufficiently small. A current I occurs so that the capacitance formed by the two electrodes is shortcircuited: the voltage at R_2, $V_{R_2} = R_2 \cdot I$, is sufficiently high so that $V_{C'} = 0$. Due to the current and to the potential it was not possible to obtain a stable emitter in vacuum.

We performed experiments with V positive and negative so that emission of electrons or ions occurs. The value of the field that we found, E_c = 70 kV/cm, was lower than the predicted E_c = 75 kV/cm, with the properties of mercury that can be found in literature (ρ = 13.5 g/cm^3, S = 0.45 N/m) an optical measurement of the surface tension gave a significantly lower value in air (S = 0.37 N/m, corresponding to the value given by Taylor and McDewan [3]. Because the bath was filled in air without special preparation it can explain the value of S in vacuum and therefore the value of the critical field.

The non-stabilization and the emission of the peaks kill the field by a short circuit. Once the field is zero, the instability tends to disappear and the current therefore stops. If the power supply is still connected the field builds up again and the instability can grow another time.

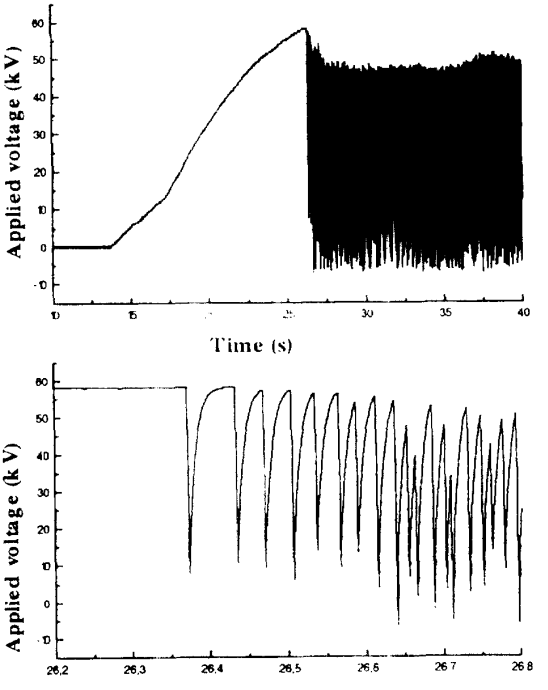

Figure 6.

Typical evolution of the voltage (b = 8 mm).

This gives an oscillatory behavior that can be observed from the voltage measured by an oscilloscope (Figure 6). After some time one can see an oscillatory pattern with a given wavelength (Figure 5(c)). Increasing the voltage then shortens the wavelength once the oscillatory behavior has taken place.

It is also seen that the phenomenon has hysteresis: the oscillatory pattern, once obtained, continues to exist with an applied voltage lower than the critical voltage (Figure 5(d)). A similar effect on gallium was reported by others [12]. These authors further showed that the

EHD instability in planar geometry is stabilized by a transverse magnetic field that is typically found in ion diodes.

3.2. CONFINED GEOMETRY

For a confined geometry, *i.e.* the radius of the bath is of the order or less than the wavelength which corresponds for mercury to a diameter < 1 cm, one does not see a real pattern but a small number of peaks. The confinement makes the destabilization more difficult when the liquid is properly anchored at the lateral walls because the wavelength must fit the bath. The critical field is then higher (Table 1) and a stable non-emitting deformed interface can be observed. A stable emitting surface was not obtained in vacuum (due to the current as explained above).

Table 1.
Critical onset field E for small radii R of the bath.

R, cm	E, kV/cm
0.10	132
0.15	112
0.20	100
0.25	86
0.30	82
0.35	77
0.40	77
0.50	70
4.00	70

A rigorous calculation of the critical field for a radius R has been performed elsewhere [9]. The corresponding law fits well with the following form

$$E_c(R)^2 = E_c(\infty)^2 \left[1 + \left(\frac{\xi_0}{R}\right)^2\right] \qquad (18)$$

where ξ_0 is a parameter (coherence length) of the order of l_c and $E_c(\infty)$ the critical field in unbounded geometry. It is possible to observe that this deformation corresponds to a displacement of the surface combination of functions of the type $J_m(kr)\cos(m\theta)$ where J_m is the usual Bessel function of the first kind. For small baths a single value of m leads to a solution approaching the complete solution: a critical field $E_c(m, R)$ can be attached to each mode. If the fields are not equal the onset is reached for a given m, corresponding to $\min(E_c(m, R))$. In this case m is the number of peaks and $m = 1$ is the first mode to be destabilized for small radii.

We have plotted in Figure 7
$y = 1/2\ln\{[E_c(R)/E_c(R=\infty)]^2 - 1\}$ *vs.* $x = \ln(R)$, with experimental and calculated data.

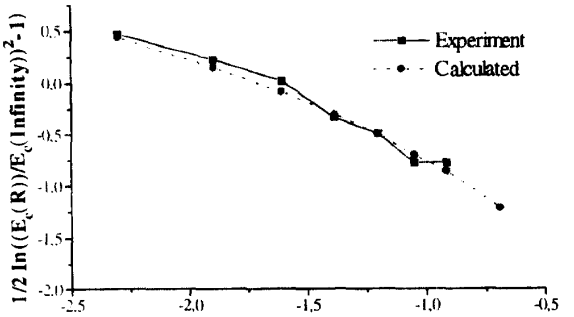

Figure 7.

Critical field E_c versus radius R of the bath in logarithmic plot.

Equation (18) corresponds to $y = \ln(\xi_0) - x$ and a linear regression gives $y = \ln(0.18) - 0.98x$. So it gives $\xi_0 \approx l_c = 0.17$ cm.

For higher values of the field, the curvature becomes large enough and is not stable any more. The apex becomes significantly thiner and then begins to emit.

A pattern can be observed on a large bath which appears for the well-known critical field of unbounded geometry. A small number of peaks appear for a small bath at a new and higher critical field $E_c(R)$, we then found a stable deflected surface. An intermediate case occurs for diameters that only allow a small number of peaks but for which the critical field is approximately equal to the one of the infinitely large case (diameter=1 cm). In this case no stabilization of the emitter has been observed in vacuum for our values of b. In very small bath ($R = 1$ mm) we found a deflection of the surface which was not directly followed by emission. For thin layers of mercury and gallium an experimental stabilization of the liquid emitter has been obtained by replacing vacuum by paraffin oil: the current is then sufficiently small so that the electric field still exists.

4. CONCLUSION

THE destabilization of a liquid interface by a normal electric field fits well with the usual linear theory. However, the effects of the lateral geometry can affect the critical value. For very small sizes of the bath the field necessary to obtain a deflection of the liquid surface is significantly higher. The pattern was obtained thanks to the boundary conditions: anchorage of the fluid on the lateral bath boundaries and volume conservation; it prevents a destabilization of zeroth order before onset. Stabilization of the pattern was not observed in vacuum due to the current emission that killed the field, and instead an oscillatory behavior takes place: this prevents a full pattern of sharp peaks to be obtained. We observed

that, once it has appeared, the instability grows until emission, except in a very confined geometry.

ACKNOWLEDGMENT

We would like to thank H. González for the theoretical aspect, R. Brimaud and F. Barata for the technical part of the experiment, and S. Assal for interesting discussions.

REFERENCES

[1] L. Tonks, "A Theory of Liquid Surface Rupture by a Uniform Electric Field", Phys. Rev., Vol. 48, pp. 562–568, 1936.

[2] Ya. I. Frenkel, "Tonks Theory of Liquid-surface Rupture by a Constant Electric Field in Vacuo", Zh. Eksp. Teor. Fiz., Vol. 6, p. 347, 1936.

[3] G. I. Taylor and A. D. McDean, "The Stability of a Horizontal Fluid Interface in a Vertical Electric Field", J. Fluid Mech., Vol. 22, pp. 1–15, 1965.

[4] J. R. Melcher, "Electrohydrodynamic and Magnetohydrodynamic Surface Waves and Instabilities", Phys. Fluids, Vol. 4, pp. 1348–1354, November 1961.

[5] J. R. Melcher, *Continuum Electromechanics*, Chapter 8. The MIT Press, Cambridge, 1981.

[6] V. A. Nevrovskii, "Instability of Molten-metal Film in an Electric Field", Izvestiya Akademii Nauk SSSR, Mekhanica Zhidkosti i Gaza., Vol. 4, pp. 20–28, 1977.

[7] J. He, N. M. Miskovski, P. H. Cutler and M. Chung, "Effects of Viscosity on Capillary Wave Instability of a Planar Liquid-metal Surface in an Electric Field", J. App. Phys., Vol. 68, pp. 1475–1482, August 1990. Their Equation (33) is different from our relation (3), which is equivalent only for thick films, because of a sign error in the determinant.

[8] G. Néron de Surgy, J.-P. Chabrerie, O. Denoux and J.-E. Wesfreid, "Linear Growth of Instabilities on a Liquid Metal under Normal Electric Field", J. Phys. II France, Vol. 3, 1201–1225, August 1993.

[9] A. L. Pregenzer and B. M. Marder, "Liquid Lithium Ion Source: Nonlinear Behavior of Liquid Surface in Electric Field", J. Appl. Phys., Vol. 60 (11), 3821–3824, December 1986.

[10] E. A. Kuznetsov and M. D. Spektor, "Existence of a Hexagonal Relief on the Surface of a Dielectric Fluid in an External Electric Field", Sov. Phys. JETP, Vol. 44, pp. 136–141, 1976.

[11] A. Gailitis, "Formation of the Hexagonal Pattern on the Surface of a Ferromagnetic Fluid in an Applied Magnetic Field", J. Fluid Mech., Vol. 82, pp. 401–413, 1977.

[12] C. Mayberry, E. Schamiloglu, and C.W. Mendel Jr., "Long Pulse Ion Diode for Planar Electrohydrodynamic Instability Studies", IEEE International Conference on Plasma Science, Williamsburg, VA, 1991.

This paper is based on a presentation given at the 16th International Symposium on Discharges and Electrical Insulation in Vacuum, Moscow, Russia, 1994.

Manuscript was received on 14 August 1994, in final form 18 January 1995.